ORGANIC PROCESS RESEARCH & DEVELOPMENT
OPR&D

pubs.acs.org/OPRD

Article

Development of Two Synthetic Approaches to an APJ Receptor Agonist Containing a Tetra-*ortho*-Substituted Biaryl Pyridone

Matthew J. Goldfogel,* Christopher R. Jamison, Scott A. Savage, Matthew W. Haley, Subha Mukherjee, Chris Sfouggatakis, Manjunath Gujjar, Jayaraj Mohan, Souvik Rakshit, and Rajappa Vaidyanathan

Cite This: https://doi.org/10.1021/acs.oprd.1c00088

Read Online

ACCESS | Metrics & More | Article Recommendations | Supporting Information

ABSTRACT: The development and implementation of two process syntheses to provide **BMS-986224**, an agonist of the APJ receptor, are reported. The first-generation synthesis of **BMS-986224** relied on a key enamine cyclization to construct the pyridone core; however, the overall efficiency of this route was limited by the linear synthesis of the hindered biaryl pyridone. This lack of convergence is solved in a second-generation route that minimizes low-temperature lithiation chemistry, replaces costly Pd coupling with scalable nucleophilic arylation, and reduces step count. The improved synthesis was enabled by a new Negishi coupling method that addresses limitations of the Suzuki−Miyaura literature for tetra-*ortho*-substituted biaryl pyridones.

KEYWORDS: *process synthesis, heart failure, APJ receptor agonist, Negishi coupling, tetra-ortho-substituted heteroarene*

Heart failure is a chronic disease diagnosed in more than 24 million people worldwide each year and currently affects over 5 million patients within the United States.[1,2] Some severe cases present as systolic heart failure (or HFrEF), where there is a reduction in the left ventricular ejection fraction by over 50%. Despite extensive pharmaceutical research and state-of-the-art medical care, only half of patients with this type of heart failure survive beyond 5 years.[3,4] This highlights the significant need for new therapeutics and treatments to assist patients living with this condition.

The APJ system plays a key role in cardiovascular regulation,[5−9] and significant effort has been devoted to the study of its endogenous peptide ligand apelin as a potential therapeutic option for treating heart failure and HFrEF.[10,11] Intraveneous administration of apelin-13 was shown to improve cardiac output with minimal increase in blood pressure or heart rate.[12−15] Unfortunately, apelin-13 rapidly degrades in the human body and is not suitable as a therapeutic for chronic treatment.[16] This promising medical proof-of-concept inspired the design and synthesis of many apelin peptide mimics and small molecule APJ agonists as potential therapeutics.[17−23] Medicinal chemistry research at Bristol Myers Squibb contributed to this field and identified a series of pyrimidinone agonists of the APJ receptor (Scheme 1A).[24] Ongoing drug development improved upon these initial hits with structure−activity relationship (SAR) studies and introduced an *ortho*-disubstituted biaryl pyridone structure to increase chemical stability.[25] This culminated in the design of **BMS-986224**, which was advanced as a clinical drug candidate.[26]

BMS-986224 is comprised of three linked arenes including a central, fully substituted pyridone. This pyridone is functionalized in the 3-position by an unusual oxadiazole with a pendant pyridylmethylene, and in the 5-position by a hindered 2,6-dimethoxyphenyl. Analog synthesis for SAR studies was accomplished through a late-stage introduction of the oxadiazole to the key biaryl pyridone core (Scheme 1B).

Scheme 1. Prior Work in Developing and Synthesizing BMS-986224 and Comparison to Process Retrosynthetic Disconnections

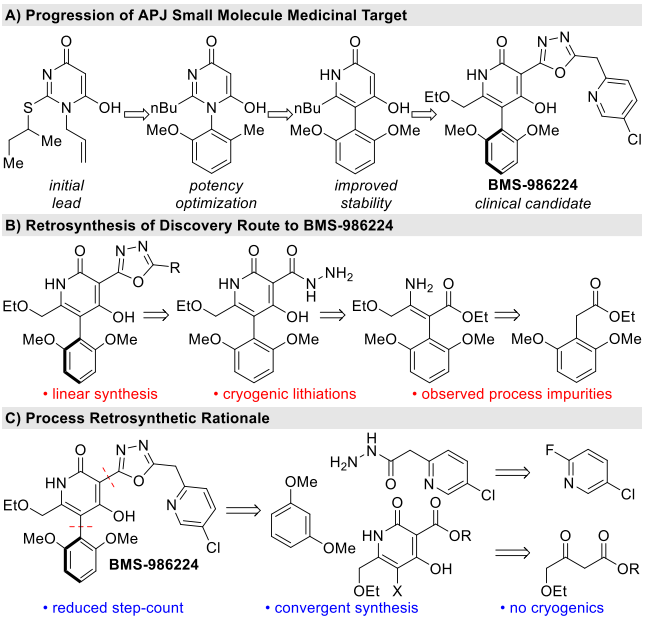

Special Issue: Excellence in Industrial Organic Synthesis 2021

Received: March 9, 2021

This heterobiarene was linearly constructed through lithiations of 1,3-dimethoxybenzene and subsequent pyridone formation via a Guareschi−Thorpe type cyclization.[27−29] While implementing this synthetic strategy on multikilogram scale to provide material for clinical studies (*vide infra*), opportunities for improvement prior to selecting a commercial process were identified: (1) route efficiency and project timelines were impacted by the linear approach to building the biaryl pyridone; (2) undesirable cryogenic lithiations were required to functionalize the 2,6-dimethoxyarene and alkylate the pyridine side-chain; and (3) formation of several process impurities complicated the isolation and purification of synthetic intermediates. Based on these key drivers, a second-generation route was designed to support further clinical supply of **BMS-986224** (Scheme 1C).

This second-generation approach required overcoming state-of-the-art cross-coupling limitations to forming the key tetra-*ortho*-substituted biaryl bond. Literature methods that employ 5-arylpyridones in cross-coupling are quite rare,[30−32] and reduced yields are routinely obtained when compared to simple arenes.[33−38] Forming the biaryl linkage in **BMS-986224** is further complicated by the sterics of the tetra-*ortho*-substitution pattern. Cross-coupling of hindered arenes remains a synthetic challenge despite the maturity of the field and is an active area of research.[39−51] To the best of our knowledge, the reported second-generation synthesis of **BMS-986224** marks the first example of forming a tetra-*ortho*-substituted biaryl pyridone via cross-coupling.

Herein are reported learnings from pilot plant-scale utilization of the first-generation synthesis (Scheme 1B) and the subsequent development of a convergent second-generation synthesis of **BMS-986224** (Scheme 1C). Additional development work focused on synthesizing the benzylic hydrazide through nucleophilic aromatic substitution of 5-chloro-2-fluoropyridine to avoid cryogenic lithiation and palladium catalysis. This second-generation route culminated with a late-stage hydrazide coupling that was performed without amide coupling agents, many of which are a safety risk due to their sensitizing properties.[52]

RESULTS AND DISCUSSION

First-Generation Synthesis. In order to rapidly supply API for toxicology and early clinical studies, the first-generation route was implemented on kilogram scale. This synthesis employed the retrosynthetic strategy highlighted in Scheme 1B which affords the biaryl pyridone core in 5 steps.

Synthesis of **BMS-986224** began with alkylation of an organocuprate, derived from 300 kg of 1,3-dimethoxybenzene **1**, using ethylbromoacetate at −60 °C (Figure 1). The reaction provided **2** in 50−72% yield. Careful temperature control from −50 to 25 °C proved necessary to avoid sudden exotherms and side products from bis-alkylation.

Compound **2** was then lithiated and the resulting enolate reacted with 2-ethoxyacetyl chloride to provide *β*-ketoester **3** in 74% assay yield. This low conversion was traced to impurities **8**, **9**, and **10** which are derived from nonselective acylation of the enolate. Additionally, oxygen exclusion to <1000 ppm was necessary to avoid generation of oxidation impurity **11**. As intermediate **3** was not crystalline, it was telescoped to enamine **4** through treatment with ammonium acetate and **4** was isolated in 69−70% in-process yield. Although the lack of crystalline intermediates between *β*-ketoester **3** and enamine **4** led to the retention of several

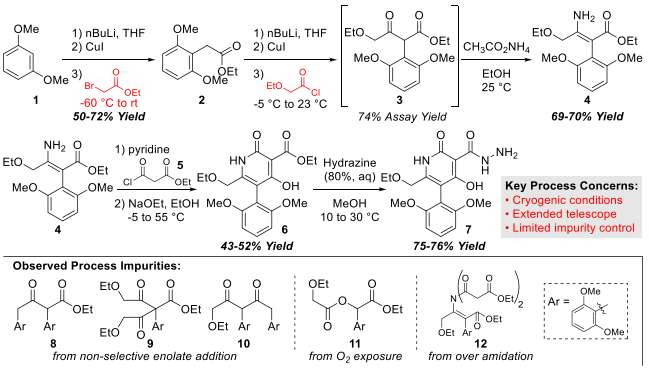

Figure 1. First-generation synthesis of biaryl pyridone core to **BMS-986224**.

impurities, the subsequent cyclization was tolerant of them and adequate purging was observed in the downstream synthesis.

Crude enamine **4** was subjected to N-acylation conditions with ethylmalonyl chloride to generate **6**. The efficiency of this reaction was pH dependent, as bis-amidation to form **12** was observed under basic conditions. This was addressed by charging ethylmalonyl chloride **5** and pyridine simultaneously to maintain a pH of 4−6, which reduced the formation of **12** to tolerable levels. (In keeping with standard industrial practice for rapid reaction analysis, in-process yields are assessed using "area percentage" (AP) yields and are uncorrected for the difference in LC response factor between the reaction components. While approximate, AP values provide insight into general trends and aid in determining improvements in reaction conversion and selectivity.) Cyclization to biaryl pyridone **6** was promoted by the addition of sodium ethoxide and crystallization of this solid from DCM and MTBE enabled the purge of impurities retained from the telescope (*vide supra*); pyridone **6** was isolated over three batches in 43−52% yield with 98.6% purity. Subsequent reaction with hydrazine hydrate provided 96.9 kg of hydrazide **7** in 75−76% yield over two batches. The hydrazide also provided excellent impurity purge and served as a quality gatekeeper of **BMS-986224**.

Synthesis of the pyridine side-chain **15** was accomplished via a two-step telescope from 2-bromo-5-chloropyridine **13** and *tert*-butyl acetate (Figure 2). Deprotonation of *tert*-butyl

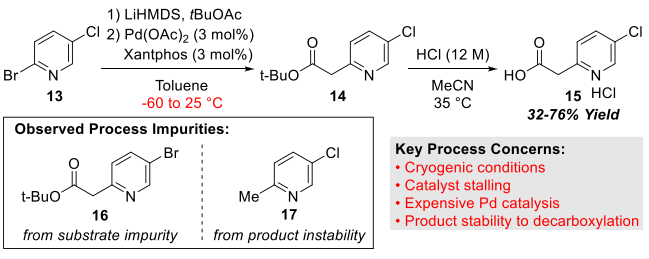

Figure 2. First-generation synthesis of pyridine side chain.

acetate with LiHMDS under cryogenic conditions and subsequent palladium-catalyzed cross-coupling with 2-bromopyridine **13** generated **14**. On scale, an unexpected bromine impurity **16** was formed due to trace quantities of 2,5-dibromopyridine present in starting material **13**. This impurity proved inseparable from the desired product, but was controlled through sourcing of **13** with <0.15 wt % of the 2,5-dibromopyridine. This analytical control of input quality was critical as the bromo analogue **16** reacted downstream to

https://doi.org/10.1021/acs.oprd.1c00088
Org. Process Res. Dev. XXXX, XXX, XXX−XXX

form brominated API. Alkylation was followed by ester hydrolysis with concentrated hydrochloric acid to provide 56.7 kg of the desired pyridine benzylic acid salt **15** in three batches with 74%, 32%, and 76% yield, respectively. (The unexpectedly low yield of the second batch was caused by reaction stalling and incomplete conversion of **14** despite kicker charges of LiHMDS and *tert*-butyl acetate. This poor reactivity was traced to catalyst death due to salt impurities and/or water contamination left in the reactor following the first batch and was solved prior to the third batch by implementing a thorough reactor cleaning protocol.) An additional challenge occurred during vacuum drying, as impurity **17** was generated during prolonged drying at 50 °C. This impurity arose from decarboxylation of **15** and was avoided by drying at reduced temperature and instituting long-term storage at <10 °C.

With both biaryl pyridone **7** and acid **15** in hand, the endgame synthesis of **BMS-986224** was undertaken (Figure 3). *N*-

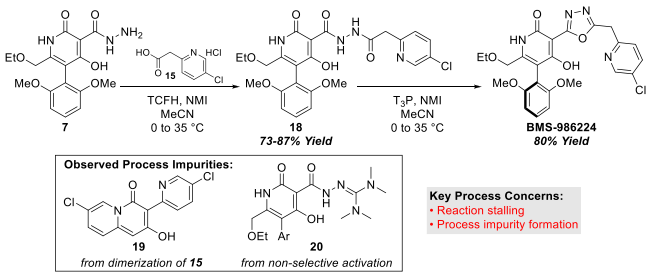

Figure 3. Amidation and cyclization endgame for first-generation synthesis of **BMS-986224**.

Acyl hydrazide formation with acid **15** was accomplished using the peptide coupling reagent *N*,*N*,*N*′,*N*′-tetramethylchloroformamidinium hexafluorophosphate (TCFH) with *N*-methylimidazole (NMI) as a base.[53] This process provided **18** in 73−87% yield, but full conversion was not reached despite additional kicker charges of TCFH or acid **15**. The incomplete conversion was caused by entrapment of the starting material during spontaneous crystallization of the product. This insoluble material was then unable to react with the TCFH present in the solution phase. The reaction was further complicated by dimerization of **15** to form impurity **19**, and unproductive TCFH activation of **7** to form impurity **20**. Fortunately, recrystallization from DCM and MeOH effectively purged these impurities and residual acid **7**. Post-campaign optimization found that starting material encapsulation could be avoided by using DMF as a cosolvent to enable a homogeneous reaction stream following TCFH addition. Use of water as an antisolvent eliminated the need for a recrystallization from DCM/MeOH and enabled a direct isolation of **18**. The improved amidation reliably afforded **18** in >95% yield and reduced the PMI from 102 to 14.

The API step proceeded uneventfully with little deviation from the discovery procedure. Cyclization of *N*-acyl hydrazide **18** to form the oxadiazole was accomplished by cyclodehydration with T_3P and provided 71.5 kg of **BMS-986224** in 80% yield. Overall, the first-generation route generated API in 10% yield over 9 transformations with a longest linear sequence of 7 steps. The cumulative process mass intensity (PMI) of the synthesis was 1,160, with the biaryl pyridone core accounting for 5 out of 9 steps with 71% of the total PMI.[54−56]

Second-Generation Synthesis. The high linearity and PMI of the first-generation synthesis, the need for cryogenic enolate conditions, and the formation of unexpected process impurities drove the development of a second-generation route to **BMS-986224**. The first-generation approach prepared intermediate biaryl pyridone **6** in a 5-step linear sequence in 14.8% overall yield. A more convergent second-generation approach would break **BMS-986224** into three components with key disconnections of cross-coupling and amidation (Figure 4). The pyridone core would be generated from

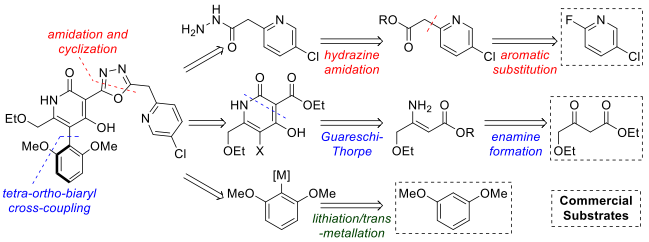

Figure 4. Synthetic strategy and commercial starting materials for second-generation synthesis.

commercially available ethyl 4-ethoxy-3-oxobutanoate via a modified Guareschi−Thorpe cyclization with diethyl malonate, while the 5-chloropyridine side chain would be prepared via an S_NAr reaction between a stabilized enolate and 2-fluoro-5-chloropyridine. This eliminated the need for cryogenic conditions and removed palladium catalysis from the side chain synthesis. Reduction in the step count would be accomplished by reversing the hydrazide coupling partners to shift hydrazide formation out of the longest linear sequence.

Implementation of this route faced the significant challenge of cross-coupling a tetra-*ortho*-substituted heterocyclic biarene containing acidic O−H and N−H bonds. In fact, earlier internal efforts to form this biaryl linkage via Suzuki-Miyaura coupling failed and were abandoned in favor of the cuprate alkylation employed in the first-generation route. As such, the development of a method for cross-coupling 5-halo-pyridones would enable our second-generation route to **BMS-986224** and fill a gap in current methodology.

Testing this key cross-coupling disconnection required isolation of the proposed 5-bromopyridone coupling partner **24** (Figure 5). Synthesis of **24** began with treatment of 4-

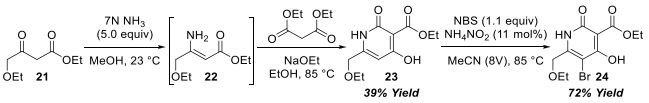

Figure 5. Second-generation synthesis of pyridone core.

ethoxy-3-oxobutanoate with 7 N ammonia in MeOH under anhydrous conditions to form intermediate **22**. Telescoped cyclization of **22** with diethyl malonate in the presence of sodium ethoxide then provided pyridone **23** in 39% yield over two steps on 170 g scale.[57−60] This improved upon the Guareschi−Thorpe strategy used in the first-generation synthesis by removing the stepwise amidation of the enamine with an acyl chloride and reducing the PMI from 230 to 55. Cross-coupling substrate **24** was prepared by bromination of the 5-position of **23** with *N*-bromosuccinimide in the presence of catalytic NH_4NO_2.[24,61] This provided 5-halopyridine **24** in 72% yield with a PMI of 29.

https://doi.org/10.1021/acs.oprd.1c00088
Org. Process Res. Dev. XXXX, XXX, XXX−XXX

With the prospective aryl bromide **24** in hand, a broad survey of cross-coupling conditions was undertaken using organometallic coupling partners 2,6-dimethoxyphenylboronic acid (Suzuki−Miyaura), 2,6-dimethoxyphenylmagnesium chloride (Kumada), and 2,6-dimethoxyphenzylzinc chloride (Negishi). High throughput experimentation (HTE) was used to survey the reaction space for each nucleophile by varying ligand, solvent, temperature, and base.[62,63] As observed by our discovery group, all attempts at Suzuki−Miyaura or Kumada coupling failed to provide **6** under any conditions. (The difficulty of this Suzuki−Miyaura coupling was further confirmed by testing phenylboronic acid as an unhindered analog of 2,6-dimethoxyphenylboronic acid—despite the removal of the tetra-*ortho*-biaryl substitution pattern, cross-coupling still occurred in <20 AP.) However, Negishi coupling with 1,3-dimethoxyphenylzinc chloride provided **6** in moderate conversion (Figure 6A). Further screening showed that

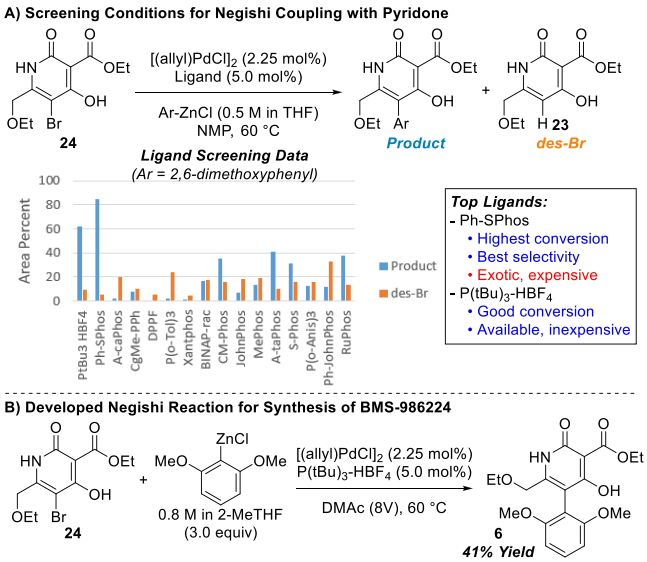

Figure 6. Discovery and development of a Negishi coupling method for synthesizing biaryl pyridone **6**.

homogeneous reactions were obtained with amide solvents and that the optimal reaction temperature was 60 °C; higher temperatures resulted in protodebromination to **23**, while lower temperatures reduced conversion. Ligand identity had the greatest effect on product and side-product formation, and Ph-SPhos and $P(tBu)_3$-HBF_4 were selected for further study on the basis that they provided >60 AP **6** with minimal protodebromination.

Further development was undertaken to translate the HTE screening conditions to a gram-scale process. Scalable preparation of the organometallic coupling reagent 2,6-dimethoxyphenylzinc chloride was accomplished via lithiation followed by transmetalation to $ZnCl_2$ at 0 °C. Initial reaction conditions employed THF as a solvent but resulted in inconsistent yields due to super saturation of the LiCl byproduct and uncontrolled precipitation during reagent storage. This was solved by switching the reaction solvent to 2-MeTHF to reduce the solubility of LiCl and enable removal by filtration. Additionally, the cross-coupling was improved by replacing the solvent *N*-methyl-2-pyrrolidone (NMP) with *N*,*N*-dimethylacetamide (DMAc) to allow the use of $P(tBu)_3$-HBF_4 as a more cost-effective ligand and increase the reaction concentration.

These optimizations culminated in the process shown in Figure 6B, where **6** was generated by reacting 5-bromo-pyridone **24** with 2,6-dimethoxyphenylzinc chloride. The presence of excess 1,3-dimethoxybenzene (generated from quenching the arylzinc reagent) complicated crystallization, but acidifying the reaction stream allowed for the removal of this impurity by heptane wash. Subsequent extraction with EtOAc, solvent swap to iPrOH, and crystallization with water provided **6** in 41% yield with a PMI of 150. To our knowledge, this is the first example of forming a tetra-*ortho*-substituted biarylpyridine through cross-coupling and demonstrates how access to this new disconnection can significantly improve process efficiency.

After completion of the biaryl pyridone core, focus turned to the synthesis of the side-chain hydrazide **32**. In particular, a route that could access **32** without the use of palladium catalysis to generate the carbon−carbon bond between the acetate and the heteroaryl moieties was desired as a cost reducing measure. The feasibility of an uncatalyzed carbon−carbon bond formation via nucleophilic aromatic substitution was evaluated on 2-fluoro-5-chloropyridine **25** with a panel of nucleophiles including acetonitrile, *tert*-butyl acetate, diethyl malonate, Meldrum's acid, and *tert*-butyl cyanoacetate (**26**). From this study, *tert*-butyl cyanoacetate was selected as optimal due to its high nucelophilicity, clean reaction profile, and the crystallinity of the resultant adduct **27**. Scale up demonstrated that **25** reacted with **26** and potassium carbonate at 120 °C in DMF to form pyridine **27** in 57% isolated yield after crystallization from DMF and water (Figure 7A).

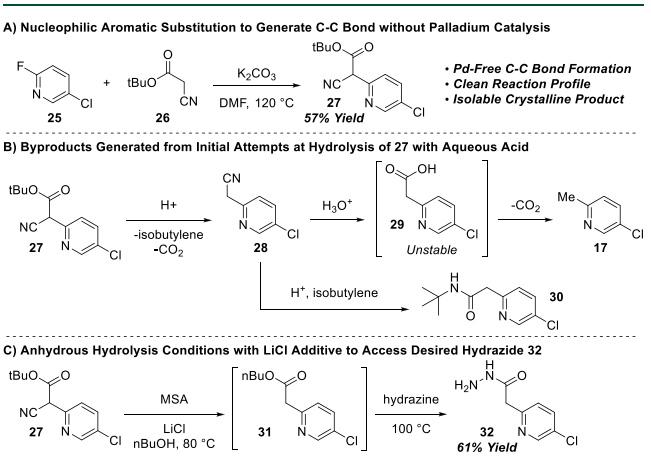

Figure 7. Palladium-free synthesis of the hydrazide side chain **32**.

Despite the attractive features of the synthesis, initial attempts to convert **27** to hydrazide **32** proved troublesome, as has been previously reported in the literature for hydrolysis of such *tert*-butyl cyanoacetate adducts.[64] Hydrolysis of **27** with aqueous acid resulted in the formation of side products **17** and **30** (Figure 7B). Methylpyridine **17** resulted from overdecarboxylation of the unstable acid intermediate **29** under highly acidic conditions, whereas *tert*-butyl amide **30** was generated via a Ritter reaction between intermediate nitrile **28** and the isobutylene liberated from the acid-mediated decarboxylation of *tert*-butyl ester **27**. Despite initial setbacks, it was found that the desired transformation of **27** to **32** could

https://doi.org/10.1021/acs.oprd.1c00088
Org. Process Res. Dev. XXXX, XXX, XXX−XXX

be accomplished with anhydrous methanesulfonic acid and LiCl in *n*-butanol (Figure 7C). Anhydrous conditions were necessary to suppress overdecarboxylation to methylpyridine **17** by protecting the unstable acid moiety as *n*-butyl ester **31**. The LiCl additive was included to minimize formation of the Ritter byproduct **30** by trapping the *tert*-butyl carbocation generated during decarboxylation. Clean formation of the intermediate *n*-butyl ester **31** was followed by a telescoped hydrazide formation to form **32**, which was isolated via crystallization from *n*-butanol in 61% yield with a PMI of 33 for the telescope. Overall, the second-generation synthesis of side-chain **32** was accomplished in 35% yield from 2-fluoro-5-chloropyridine without the need for cryogenic conditions, palladium catalysis, or peptide coupling reagents.

Completion of **BMS-986224** via our second-generation synthesis relied on the condensation of hydrazide **32** and biaryl ester **6** (Figure 8). Formation of the *N*-acyl hydrazide **18**

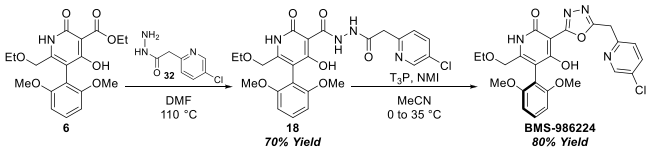

Figure 8. Hydrazide formation and oxadiazole cyclization in second-generation synthesis.

occurred readily at 110 °C in DMF without the need for a peptide coupling reagent. This unusual and efficient amidation is possible due to the nucleophilicity of the hydrazide and corresponding electrophilic activation of the ester by the electron poor pyridone ring. Reaction of **6** and **32** provided the product **18** in 70% yield with a PMI of 18. **BMS-986224** was accessed from **18** via the unaltered first-generation protocol without any changes to the purity profile or yield (80%).

Overall, the second-generation route enabled the synthesis of **BMS-986224** in 8 steps with a longest linear sequence of 6 steps (Table 1). This required only 7 isolations and removed

Table 1. Comparison of First and Second Generation Synthetic Routes

	First Generation	Second Generation
Step Count	9	8
Longest Sequence	7	6
Cryogenic Steps	3	0
PMI	1,160	413
Overall Yield	10%	6.4%

all cryogenic steps. The route provided a yield of 6.4% and a cumulative PMI of 413, which is nearly a 3-fold improvement over the first-generation route.

CONCLUSION

Two synthetic routes to **BMS-986224** are reported. The first route was used to rapidly deliver 71.5 kg of API with a PMI of 1,160. Focusing on speed to patient, initial deliveries fulfilled early clinical needs via a near-linear route. In preparation for Phase II trials, an improved second-generation route was developed to (1) remove multiple cryogenic lithiations, (2) reduce the formation of process impurities, and (3) reduce the longest linear sequence. This convergent second-generation route was made possible by disconnecting the tetra-*ortho*-substituted biaryl pyridone through a newly enabled Negishi coupling. This disconnection was not possible using traditional Suzuki−Miyaura conditions, and this report details the first use of cross-coupling to form a tetra-*ortho*-substituted biaryl pyridone. The second-generation synthesis improved the synthesis of the pyridyl side chain by forming it through aromatic substitution in place of expensive palladium catalysis. Overall, the improved route was demonstrated on gram scale to reduce the PMI to 413 and will be used to enable any future kilogram-scale campaigns.

EXPERIMENTAL SECTION

General Considerations. All starting materials, reagents, and solvents were purchased from commercial suppliers and used as received unless indicated. All reactions were performed under a nitrogen atmosphere with <0.1% oxygen unless otherwise specified. ^{1}H NMR (400 MHz) and ^{13}C NMR spectra were measured on a Bruker AVANCE 400 at 400 MHz for proton and 100 MHz for carbon, and chemical shifts are reported in parts per million using the residual solvent peak as a reference. LC-MS analysis was performed on a Shimadzu LCMS-2020 mass spectrometer primarily using an Agilent Poroshell 120 EC-C18 column (2.1 mm × 50 mm, 1.9 μm) and HRMS samples were run on an Agilent 6230B LC-ToF (see the Supporting Information for more details on the respective spectra).

Preparation of Ethyl 2-(2,6-Dimethoxyphenyl)acetate (2). A dried titanium reactor under positive nitrogen pressure was charged with THF (873 kg) and 1,3-dimethoxybenzene (100.2 kg, 1.0 equiv) before being cooled to 10−20 °C. A solution of 2.5 M *n*-BuLi in hexanes (221.5 kg, 1.1 equiv) was charged slowly while maintaining a temperature of <20 °C, and the reaction was agitated for 1 h. CuI (76.9 kg, 0.55 equiv) was added, and the mixture was agitated at 20 °C for 1 h. The reaction was cooled to −80 °C, and ethyl bromoacetate (132.2 kg, 1.1 equiv) was charged slowly while maintaining a temperature below −60 °C. The reaction was warmed to −45 °C and agitated for 12.5 h before being warmed to 20 °C. Water (799 kg) was slowly added to quench the reaction stream at 10−20 °C. The reaction mixture was filtered through Celite (50.5 kg), and the Celite was rinsed with MTBE (267.8 kg). The mother liquor was extracted with MTBE (2 × 370.5 kg), and the collected organic layer was washed with a 5% solution of ammonium hydroxide (4× 375 kg) and water (3× 503.3 kg). The organic layer was collected, and the solvent was swapped to heptane (2× 478 kg) via put-and-take distillation under reduced pressure at <50 °C with a final volume of ∼2 V (∼200 L). The product was crystallized from the heptane solution by cooling to −5 °C and agitating for >5 h. The product was isolated by filtration, and the solid was rinsed with heptane (136 kg) at −5 °C. The resulting solid was dried under reduced pressure at <30 °C to provide **2** (80.1−115.3 kg) as an off-white solid in 50−72% yield over three batches. ^{1}H NMR (400 MHz, DMSO-d_6) δ 7.23 (t, J = 8.3 Hz, 1H), 6.65 (d, J = 8.4 Hz, 2H), 4.05 (q, J = 7.1 Hz, 2H), 3.75 (s, 6H), 3.56 (s, 2H), 1.17 (t, J = 7.2 Hz, 3H). ^{13}C NMR (101 MHz, DMSO-d_6) δ 171.5, 158.4, 128.8, 111.3, 104.3, 60.3, 56.2, 28.9, 14.5. Spectra match literature characterization data.[25]

Preparation of Ethyl (*Z*)-3-Amino-2-(2,6-dimethoxyphenyl)-4-ethoxybut-2-enoate (4). A dried glass-lined reactor under positive nitrogen pressure was charged with THF (1073 kg) and **2** (100.0 kg, 1.0 equiv). The solution was sparged with nitrogen to obtain <0.1% oxygen and then cooled

https://doi.org/10.1021/acs.oprd.1c00088
Org. Process Res. Dev. XXXX, XXX, XXX−XXX

to 10 °C. A 1.0 M solution of lithium bis(trimetlysilyl)amide in THF (410.1 kg, 1.1 equiv) was charged slowly while maintaining a temperature below 20 °C, and the solution was agitated for 1 h. Ethoxyacetyl chloride (38.4 kg, 0.7 equiv) was charged slowly while maintaining a temperature below 20 °C, and the solution was allowed to stir for 1 h. The base and acyl chloride addition was then repeated by charging a 1.0 M solution of lithium bis(trimetlysilyl)amide in THF (410.2 kg, 1.1 equiv), agitating for 1 h, and then charging ethoxyacetyl chloride (38.0 kg, 0.7 equiv). The reaction mixture was agitated at 10−20 °C for 6 h before being quenched with aqueous ammonium chloride (15 wt %, 1000.3 kg). The solution was extracted with MTBE (3× 370 kg), and the organic layers were combined and washed with aqueous sodium chloride (5 wt %, 2999.8 kg). The organic layer was collected, and the solvent was swapped to ethanol (2× 790 kg) via put-and-take distillation under reduced pressure at <45 °C with a final volume of ∼2 V (∼200 L).

The intermediate solution of **3** was cooled to 10−20 °C prior to charging 4 Å molecular sieves (25.1 kg, 0.25 kg/kg wrt **2**) and ammonium acetate (149.6 kg, 4.0 equiv). The solution was allowed to stir at 20 °C for 20 h and then filtered, and the cake was rinsed with DCM (657.9 kg). The mother liquor and filtrate were collected, and the solvent was swapped to DCM (1330.9 kg) via distillation under reduced pressure at <45 °C with a final volume of ∼3 V (∼300 L). The resulting solution was diluted with DCM (1330.9 kg) before being washed with aqueous sodium bicarbonate (10 wt %, 2× 1003 kg) and water (500 kg). The organic layers were collected, and the solvent swap to DCM (3× 655 kg), via put-and-take distillation under reduced pressure at <45 °C to ∼2 V (∼200 L), was repeated to minimize residual ethanol. This provided **4** (850.0 kg, 11.3 wt %) as a brown solution in 69.0−70.2% in-process yield over three batches. ^{1}H NMR (400 MHz, D_2O-d_2) δ 7.16 (t, J = 8.4 Hz, 1H), 6.57 (d, J = 8.4 Hz, 2H), 3.87 (q, J = 7.1 Hz, 2H), 3.64−3.57 (m, 7H), 3.26 (q, J = 6.9 Hz, 2H), 1.03 (t, J = 7.0 Hz, 3H), 0.96 (t, J = 7.0 Hz, 3H). ^{13}C NMR (101 MHz, DMSO-d_6) δ 169.1, 159.0, 158.3, 128.7, 113.9, 104.3, 85.4, 67.8, 66.1, 58.1, 55.9, 15.2, 15.0. Spectra match literature characterization data.[25]

Preparation of Ethyl 5-(2,6-Dimethoxyphenyl)-6-(ethoxymethyl)-4-hydroxy-2-oxo-1,2-dihydropyridine-3-carboxylate (6). A dried glass-lined reactor under positive nitrogen pressure was charged with DCM (903.4 kg) and a solution of **4** in DCM (∼11.3 wt %, 849.0 kg, 1.0 equiv). The reaction was cooled to −5 °C, and a solution of pyridine in DCM (22 wt %, 178.0 kg, 1.4 equiv) and ethyl malonyl chloride in DCM (50 wt %, 183.7 kg, 1.6 equiv) were charged simultaneously to maintain a pH of 4−7 during the addition. The reaction was agitated at −5 °C for 5 h before being quenched with an aqueous solution of sodium bicarbonate (9 wt %, 909.1 kg) while maintaining a reaction temperature <20 °C. The organic layer was collected and washed with aqueous sodium bicarbonate (9 wt %, 899.6 kg) and water (958.0 kg). The organic phase was collected, and the solvent was swapped to ethanol (636.0 kg) via distillation under reduced pressure at <45 °C with a final volume of ∼2.5 V (∼250 L). The resulting solution was cooled to 20 °C and charged with ethanol (430.3 kg) and sodium ethoxide in ethanol (>18 wt %, 201.9 kg, 2.0 equiv) before being allowed to stir at 30 °C for 8 h. The reaction mixture was concentrated under reduced pressure at <45 °C to ∼2.5 V (∼250 L) before being diluted with DCM (1808 kg). The resulting solution was washed with aqueous hydrochloric acid (2 wt %, 2× 413 kg) and water (955.0 kg) before being solvent swapped to MTBE (980.4 kg) via distillation under reduced pressure at <45 °C and concentrated to ∼2.5 V (∼250 L). The product was crystallized by cooling the reaction mixture to 0 °C for 8 h. The solids were isolated by filtration and rinsed with MTBE (299.9 kg) prior to being dried under reduced pressure at <45 °C to provide **6** (50.6−61.2 kg) as a brown solid in 42.6−51.5% yield over three batches. ^{1}H NMR (400 MHz, MeOD-d_4) δ 7.37 (s, 1H), 6.71 (d, J = 8.3 Hz, 2H), 4.84 (m, 2H), 4.49−4.37 (m, 2H), 4.08 (s, 2H), 3.75 (s, 6H), 3.50−3.36 (m, 2H), 1.45−1.33 (m, 3H), 1.21−1.06 (m, 3H) ^{13}C NMR (101 MHz, MeOD-d_4) δ 174.6, 171.9, 161.6, 158.5, 149.0, 130.4, 107.7, 104.7, 103.6, 97.0, 66.3, 65.6, 61.4, 54.9, 13.8, 13.1. HRMS $[M + H]^+$ calcd for $C_{19}H_{23}NO_7$ 378.1547, found 378.1538.

Preparation of 5-(2,6-Dimethoxyphenyl)-6-(ethoxymethyl)-4-hydroxy-2-oxo-1,2-dihydropyridine-3-carbohydrazide (7). A dried glass-lined reactor under positive nitrogen pressure was charged with methanol (298.3 kg) and **6** (75.0 kg, 1.0 equiv). The reaction was cooled to 10−15 °C, and hydrazine hydrate (98.0 kg, 8.0 equiv) was charged slowly while maintaining a temperature of <15 °C. The reaction was warmed to 20−30 °C and allowed to stir for 5 h. The product was crystallized by cooling the solution to 0 °C for 2 h and isolated by filtration followed by cake washes with methanol (111.1 kg) and water (370.2 kg). The isolated solid was then recrystallized by dissolving in DCM (432.9 kg) and methanol (122.3 kg) at 35−40 °C before charging MTBE (579.2 kg) as an antisolvent. The resulting slurry was cooled to 20 °C and agitated for 2 h before being filtered to isolate the solid. The solid cake was rinsed with MTBE (140.7 kg) and dried under reduced pressure at <45 °C to provide **7** (54.2−55.1 kg as a white solid in 74.9−76.1% yield. ^{1}H NMR (500 MHz, DMSO-d_6) δ 15.72 (s, 1H), 11.55 (br s, 1H), 10.94 (s, 1H), 7.35 (t, J = 8.3 Hz, 1H), 6.72 (d, J = 8.4 Hz, 2H), 4.77 (br s, 2H), 3.96 (s, 2H), 3.69 (s, 6H), 3.27 (q, J = 7.0 Hz, 2H), 0.99 (t, J = 7.0 Hz, 3H). ^{13}C NMR (101 MHz, DMSO-d_6) δ 173.4, 168.9, 162.7, 158.6, 146.6, 130.6, 108.9, 106.3, 104.5, 96.8, 66.1, 65.9, 56.1, 15.2. HRMS $[M + H]^+$ calcd for $C_{17}H_{21}N_3O_6$ 364.1503, found 364.1521.

Preparation of 2-(5-Chloropyridin-2-yl)acetic Acid Hydrochloride (15). A dried titanium reactor under positive nitrogen pressure was charged with toluene (85.3 kg) and a solution of lithium bis(trimethylsilyl)amide in toluene (1.0 M, 403.7 kg, 2.5 equiv). The reaction mixture was cooled to −60 °C, and *tert*-butylacetate (50.9 kg, 2.3 equiv) was charged slowly while maintaining a temperature of −60 °C. The resulting solution was allowed to stir for 1 h at −60 °C and held at this temperature for further use.

A second dried glass-lined reactor under positive nitrogen pressure was charged with toluene (158.0 kg) and sparged with nitrogen to obtain <0.1% oxygen. Palladium acetate (1.28 kg, 3 mol %) and dimethylbisdiphenylphosphinoxanthene [xantphos] (3.3 kg, 3 mol %) were charged, and the mixture was allowed to stir at 25−30 °C for 1 h. 2-Bromo-5-chloropyridine (36.5 kg, 1.0 equiv) was charged to this solution followed by the prepared solution of lithium bis(trimethylsilyl)amide and *tert*-butylacetate. The reaction was allowed to stir at 25−30 °C for 5 h before being cooled to 10−20 °C. The crude reaction stream was washed with a solution of aqueous citric acid (17 wt %, 2× 219 kg) and water (2× 183 kg), and the organic layer was collected. The organic solution was treated with active carbon (11.0 kg) and an aqueous solution of *N*-acetyl-cysteine

https://doi.org/10.1021/acs.oprd.1c00088
Org. Process Res. Dev. XXXX, XXX, XXX−XXX

(3 wt %, 70.3 kg) and agitated for 4 h at 20−30 °C. The resulting solution was filtered, and the cake and reactor were rinsed with toluene (221.3 kg). The mother liquor was collected, and a solution of intermediate **14** was isolated in acetonitrile by solvent swapping to acetonitrile (3× 173 kg) via put-and-take distillation under reduced pressure at <55 °C with a final volume of ∼125 L.

The isolated solution of **14** in acetonitrile was telescoped into decarboxylation by charging concentrated hydrochloric acid (37 wt %, 87.1 kg) at 25 °C, and the mixture was agitated for 14 h at 25−30 °C. The product was crystallized by charging MTBE (346.3 kg), cooling the reaction mixture to −5 °C, and agitating for 6 h. The solids were isolated by filtration, and the reactor and cake were rinsed with MTBE (86.6 kg). The resulting solids were dried under reduced pressure at <30 °C to provide **15** (12.5−29.9 kg) as a light yellow powder in 73.9%, 31.6%, and 75.7% yield over three batches. The unexpectedly low yield in the second batch was the result of reaction stalling caused by water and/or salt impurities carried over in the reactor from the first batch. This was solved prior to the third batch by implementing a thorough reactor cleaning protocol. ^{1}H NMR (500 MHz, MeOD-d_4) δ 9.05 (d, J = 2.3 Hz, 1H), 8.63 (dd, J = 8.7, 2.3 Hz, 1H), 8.06 (d, J = 8.5 Hz, 1H), 5.01 (br s, 4H). ^{13}C NMR (101 MHz, MeOD-d_4) δ 168.3, 148.8, 145.5, 141.8, 133.3, 129.2. HRMS [M + H]$^+$ calcd for $C_7H_6ClNO_2$172.0160, found 172.0161.

Preparation of *N*′-(2-(5-Chloropyridin-2-yl)acetyl)-5-(2,6-dimethoxyphenyl)-6-(ethoxymethyl)-4-hydroxy-2-oxo-1,2-dihydropyridine-3-carbohydrazide (18). A dried reactor under positive nitrogen pressure was charged with acetonitrile (304.2 kg), **15** (24.1 kg, 1.2 equiv), and 1-methylimidzole (29.3 kg, 3.7 equiv) at 20−30 °C. To the agitated reaction mixture was charged **7** (35.0 kg, 1.0 equiv) followed by an acetonitrile (27.7 kg) rinse, and the reactor was cooled to 0−5 °C. A second dried reactor under positive nitrogen pressure was charged with acetonitrile (110.6 kg) and *N*,*N*,*N*′,*N*′-tetramethylchloroformamidinium hexafluorophosphate [TCFH] (31.1 kg, 1.15 equiv) before being agitated at 20−35 °C for 30 min to obtain a homogeneous solution. The prepared solution of TCFH in acetonitrile was charged to the reactor containing **7** while maintaining a temperature of 0−8 °C. The reaction mixture was agitated and allowed to stir for 4 h before the slurry was filtered, and the cake rinsed with acetonitrile (2× 110.6 kg). The solid was collected and transferred to a reactor for recrystallization using DCM (931.0 kg) and MeOH (55.4 kg) as solvents. The mixture was warmed to 31−35 °C, and MTBE (259.0 kg) was charged as an antisolvent. The reaction mixture was agitated for 1 h before filtering and rinsing the solid with MTBE (2× 103.6 kg). The resulting product was dried under reduced pressure at <55 °C to provide **18** (39.5−43.5 kg) as an off-white powder in 73.1−87.4% yield over two batches. ^{1}H NMR (400 MHz, DMSO-d_6) δ 15.00−14.88 (m, 1H), 11.94 (br s, 1H), 11.78 (s, 1H), 10.89 (br s, 1H), 8.54 (d, J = 2.4 Hz, 1H), 7.92−7.85 (m, 1H), 7.45 (d, J = 8.4 Hz, 1H), 7.35 (t, J = 8.4 Hz, 1H), 6.71 (d, J = 8.4 Hz, 2H), 3.97 (s, 2H), 3.79 (s, 2H), 3.68 (s, 6H), 3.26 (q, J = 7.0 Hz, 2H), 0.98 (t, J = 7.0 Hz, 3H). ^{13}C NMR (101 MHz, DMSO-d_6) δ 171.7, 166.4, 164.9, 160.7, 156.5, 152.5, 145.8, 145.8, 134.7, 128.6, 127.8, 123.7, 106.4, 104.2, 102.4, 94.5, 64.0, 63.8, 54.0, 40.1, 13.1. HRMS [M + H]$^+$ calcd for $C_{24}H_{25}ClN_4O_7$ 517.1485, found 517.1494.

Preparation of 3-(5-((5-Chloropyridin-2-yl)methyl)-1,3,4-oxadiazol-2-yl)-5-(2,6-dimethoxyphenyl)-6-(ethoxymethyl)-4-hydroxypyridin-2(1*H*)-one (BMS-986224). A dried reactor under positive nitrogen pressure was charged with acetonitrile (274.9 kg) and **18** (43.5 kg, 1.0 equiv) before being warmed to 20−35 °C. 1-Methylimidazole (15.2 kg, 2.2 equiv) and a solution of propylphosphonic anhydride [T_3P] (50 wt % in EtOAc, 139.2 kg, 2.6 equiv) was charged, and the reaction was warmed to 75 °C and agitated for 24 h. The resulting slurry was cooled to 20−30 °C, and water (435.0 kg) was charged as an antisolvent. The reaction was cooled to 0−5 °C and agitated for 1 h before the solids were isolated by filtration, and the cake was rinsed with a solution of acetonitrile and water (50/50 v/v, 2× 77.9 kg) and water (3× 261.0 kg). The resulting solids were dried under reduced pressure at <50 °C to provide **1** (33.8 kg) as a white, free-flowing powder in 80.4% yield. ^{1}H NMR (500 MHz, DMSO-d_6) δ 12.14−11.70 (m, 1H), 11.44 (br s, 1H), 8.56 (d, J = 2.4 Hz, 1H), 7.97 (dd, J = 8.4, 2.6 Hz, 1H), 7.55 (d, J = 8.4 Hz, 1H), 7.36 (t, J = 8.3 Hz, 1H), 6.73 (d, J = 8.4 Hz, 2H), 4.58 (s, 2H), 3.95 (s, 2H), 3.69 (s, 6H), 3.26 (q, J = 6.9 Hz, 2H), 0.98 (t, J = 6.9 Hz, 3H). ^{13}C NMR (101 MHz, DMSO-d_6) δ 168.1, 164.1, 163.4, 159.5, 158.7, 153.8, 148.3, 147.4, 137.4, 130.7, 130.4, 125.4, 109.0, 104.6, 104.5, 94.5, 66.2, 65.8, 56.2, 33.3, 15.2. HRMS [M + H]$^+$ calcd for $C_{24}H_{23}ClN_4O_6$ 499.1379, found 499.1385.

Preparation of Ethyl 6-(Ethoxymethyl)-4-hydroxy-2-oxo-1,2-dihydropyridine-3-carboxylate (23). A dried reactor under positive nitrogen pressure was charged with ethyl 4-ethoxy-3-oxobutanoate [**21**] (174.7 g, 1.0 equiv) and a solution of ammonia in methanol (7.0 M, 730 mL, 5.1 equiv) at 20−30 °C. The reaction mixture was agitated for 18 h, and the solvent was removed by azeotropic distillation with toluene (2× 400 mL) to ∼1 V. The resulting light yellow oil was filtered to remove any solids, analyzed by NMR to determine potency. Intermediate **22** (169.3 g) was isolated in 97.5% yield and telescoped into the next step without further purification.

A dried reactor under positive nitrogen pressure was charged with ethanol (1100 g), **22** (169.3 g, 1.0 equiv), and diethyl malonate (433.2 g, 3.0 equiv) at 20−30 °C. The reaction mixture was agitated, and sodium ethoxide (183.6 g, 3.0 equiv) was charged portionwise while maintaining a temperature of <35 °C. The mixture was heated to 85 °C and agitated for 22 h before being cooled to 20−30 °C. The resulting heterogeneous tan slurry was solubilized by charging water (680 mL), and the product was then crystallized via the slow addition of hydrochloric acid (1.4 M, 2080 mL) over 1 h. The resulting slurry was agitated for 1 h before the solid was isolated by filtration, and the cake was washed with water (525 mL) and MTBE (263 mL). The isolated solid was dried under reduced pressure at <55 °C to provide **23** (83.2 g) as a tan powder in 38.6% yield over two steps. ^{1}H NMR (400 MHz, $CDCl_3$) δ 13.47 (s, 1H), 10.63−10.00 (m, 1H), 5.93 (s, 1H), 4.45 (q, J = 7.1 Hz, 2H), 4.38 (s, 2H), 3.61 (q, J = 7.1 Hz, 2H), 1.44 (t, J = 7.1 Hz, 3H), 1.28 (t, J = 7.0 Hz, 3H). ^{13}C NMR (101 MHz, $CDCl_3$) δ 176.2, 172.0, 161.6, 151.1, 97.7, 97.0, 67.5, 67.2, 61.8, 15.0, 14.2. HRMS [M + H]$^+$ calcd for $C_{11}H_{15}NO_5$242.1023, found 242.1037.

Preparation of Ethyl 5-Bromo-6-(ethoxymethyl)-4-hydroxy-2-oxo-1,2-dihydropyridine-3-carboxylate (24). A dried reactor was charged with acetonitrile (54.1 g), ethyl 6-(ethoxymethyl)-4-hydroxy-2-oxo-1,2-dihydropyridine-3-carboxylate [**23**] (8.63 g, 1.0 equiv), *N*-bromosuccinimide (7.00 g, 1.1 equiv), and ammonium nitrate (0.315 g, 0.11 equiv) at 20−30 °C. The reaction mixture was agitated and warmed to

https://doi.org/10.1021/acs.oprd.1c00088
Org. Process Res. Dev. XXXX, XXX, XXX−XXX

85 °C for 2 h before being cooled to 20 °C. The product was crystallized by charging water (173 g) slowly over 4 h. The resulting slurry was filtered to isolate the solid, and the cake was rinsed with water (18 mL) and MTBE (mL). The isolated solid was dried under reduced pressure at <55 °C to provide **24** (11.5 g) as a yellow powder in 71.7% yield. ^{1}H NMR (400 MHz, $CDCl_3$) δ 14.58−14.18 (m, 1H), 9.57−8.77 (m, 1H), 4.54−4.42 (m, 4H), 3.72 (q, J = 7.0 Hz, 2H), 1.45 (t, J = 7.1 Hz, 3H), 1.33 (t, J = 7.0 Hz, 3H). ^{13}C NMR (101 MHz, $CDCl_3$) δ 172.3, 172.2, 158.8, 148.7, 97.9, 88.8, 67.7, 67.5, 62.5, 14.9, 14.2. HRMS $[M + H]^+$ calcd for $C_{11}H_{14}BrNO_5$ 320.0128, found 320.0143.

Preparation of Ethyl 5-(2,6-Dimethoxyphenyl)-6-(ethoxymethyl)-4-hydroxy-2-oxo-1,2-dihydropyridine-3-carboxylate (6). A dried reactor under positive nitrogen pressure was charged with 2-MeTHF (11.0 g), palladium(II) acetate (67.7 mg, 6.0 mol %), and tri-*tert*-butylphosphonium tetrafluoroborate (191.5 mg, 13 mol %). The resulting catalyst solution was inerted by subsurface sparge with nitrogen and agitated for 1 h at 20−25 °C. To this solution was charged DMAc (14.8 g), and ethyl 5-bromo-6-(ethoxymethyl)-4-hydroxy-2-oxo-1,2-dihydropyridine-3-carboxylate [**24**] (1.61 g, 1.0 equiv) and the resulting slurry were agitated at 20−25 °C for 30 min until fully homogeneous. A solution of 2,6-dimethoxyphenylzinc chloride in 2-MeTHF (0.92 M, 16.1 mL, 3.0 equiv) was charged slowly to the reaction mixture while controlling the mild exotherm to maintain a reaction temperature <50 °C. The reaction mixture was then warmed to 60 °C and agitated for 20 h. After reaction completion, the solution was washed with heptane (13.5 g) in three portions and acidified with 3 M hydrochloric acid (3.44 mL) before being extracted with EtOAc (30.85 g) in three portions. The organic extracts were combined and washed with saturated brine (23.5 wt % NaCl, 7.53 g) in three portions and water (1.66 g). The resulting solution was solvent swapped to iPrOH (2.49 g) and warmed to 50 °C to obtain a homogeneous solution. The product was crystallized from the solution by charging water (6.40 g) as antisolvent over 2 h and cooling the reaction mixture to 20 °C. The product was then isolated by filtration and washed with water (3.2 mL). The resulting solid was recrystallized by dissolving in iPrOH (2.49 g) at 60 °C and cooling to 20 °C to form a suspension of white solid in a light orange solution. The product was then isolated by filtration and washed with iPrOH (1.64 g) and water (3.20 g) before being dried in a vacuum oven for 18 h at 45 °C to provide **6** (768 mg) as an off-white powder in 41.3% yield and 97.8% potency. ^{1}H NMR (400 MHz, MeOD-d_4) δ 7.37 (s, 1H), 6.71 (d, J = 8.3 Hz, 2H), 4.84 (m, 2H), 4.49−4.37 (m, 2H), 4.08 (s, 2H), 3.75 (s, 6H), 3.50−3.36 (m, 2H), 1.45−1.33 (m, 3H), 1.21−1.06 (m, 3H) ^{13}C NMR (101 MHz, MeOD-d_4) δ 174.6, 171.9, 161.6, 158.5, 149.0, 130.4, 107.7, 104.7, 103.6, 97.0, 66.3, 65.6, 61.4, 54.9, 13.8, 13.1. HRMS $[M + H]^+$ calcd for $C_{19}H_{23}NO_7$ 378.1547, found 378.1538.

Preparation of *tert*-Butyl 2-(5-Chloropyridin-2-yl)-2-cyanoacetate Hydrochloride (27). A dried reactor under positive nitrogen pressure was charged with DMF (142 g), 5-chloro-2-fluoropyridine [**25**] (25.0 g, 1.0 equiv), *tert*-butyl 2-cyanoacetate [**26**] (59.6 g, 2.2 equiv), and potassium carbonate (68.3 g, 2.6 equiv) at 20−30 °C. The mixture was agitated and warmed to 120 °C for 24 h before being cooled to 20 °C. The reaction mixture was filtered to remove insoluble carbonate salts, and the reactor and cake were rinsed with DMF (189 g). The mother liquor was collected, and the product was crystallized by charging water (400 g) and hydrochloric acid (1.0 M, 140 mL). The resulting slurry was filtered to isolate the solid, and the cake was washed with a solution of DMF in water (40/60 v/v, 50 mL) and water (200 mL). The solid was dried under reduced pressure at <60 °C to provide **27** (27.5 g) as a yellow powder in 57% yield. ^{1}H NMR (400 MHz, $CDCl_3$) δ 14.37−13.94 (m, 1H, enol tautomer), 7.57 (dd, J = 6.1, 1.9 Hz, 1H), 7.45 (dd, J = 9.6, 2.3 Hz, 1H), 7.27 (s, 1H), 1.53 (s, 9H). ^{13}C NMR (101 MHz, $CDCl_3$) δ 170.4, 154.3, 139.8, 131.6, 121.5, 118.8 (d, J = 2.2 Hz, 1C), 81.6, 64.9, 28.5, 27.8. HRMS $[M + H]^+$ calcd for $C_{12}H_{13}ClN_2O_2$ 253.0738, found 253.0738.

Preparation of 2-(5-Chloropyridin-2-yl)acetohydrazide (32). A dried reactor under positive nitrogen pressure was charged with *n*-butanol (80 mL), lithium chloride (6.2 g, 3.7 equiv), and *tert*-butyl 2-(5-chloropyridin-2-yl)-2-cyanoacetate hydrochloride [**27**] (10.0 g, 1.0 equiv), and the mixture cooled to 20 °C. Methanesolufonic acid (19.0 g, 5.0 equiv) was slowly added to the reaction mixture while maintaining a temperature of <40 °C. The reaction mixture was then warmed to 80 °C and agitated for 5 h. The solution was cooled to 10 °C and diluted with *n*-butanol (40 mL) before being slowly quenched with a saturated aqueous solution of sodium carbonate (40 mL) while maintaining a temperature of <15 °C. The organic layer was collected and washed with water (2× 30 mL) before being dried by azeotropic distillation under reduced pressure at <50 °C to ∼10 V (∼100 mL) to provide a solution of intermediate butyl 2-(5-chloropyridin-2-yl)acetate [**31**]. Hydrazine monohydrate (3.2 g, 1.6 equiv) was charged, and the reaction was warmed to 100 °C before agitating for 24 h. The reaction mixture was slowly cooled to 10 °C to crystallize the product and agitated for 1 h prior to filtration. The isolated solid was rinsed with *n*-butanol (40 mL) and dried under reduced pressure at <55 °C to provide **32** (4.5 g) as a tan crystalline solid in 61% yield. ^{1}H NMR (400 MHz, MeOD-d_4) δ 8.47 (d, J = 2.3 Hz, 1H), 7.80 (dd, J = 8.4, 2.5 Hz, 1H), 7.40 (d, J = 8.3 Hz, 1H), 4.85 (s, 7H), 3.68 (s, 2H). ^{13}C NMR (101 MHz, MeOD-d_4) δ 169.9, 153.8, 147.4, 136.7, 130.5, 125.0, 41.7. HRMS $[M + H]^+$ calcd for $C_7H_8ClN_3O$ 186.0429, found 186.0431.

Second-Generation Preparation of *N*′-(2-(5-Chloropyridin-2-yl)acetyl)-5-(2,6-dimethoxyphenyl)-6-(ethoxymethyl)-4-hydroxy-2-oxo-1,2-dihydropyridine-3-carbohydrazide (18). A dried reactor under positive nitrogen pressure was charged with DMAc (15.2 mL) and **6** (1.90 g, 1.0 equiv) and agitated at 20−30 °C. To the reaction mixture was charged **32** (1.16 g, 1.2 equiv). The reaction was sealed, and the headspace was purged with nitrogen before warming to 110 °C and agitating for 24 h. The reaction was cooled to 20 °C, and water (7.60 mL) was charged to the reaction mixture to selectively precipitate an impurity. The insoluble material was removed by filtration, and additional water (3.8 mL) was charged as antisolvent to crystallize the product. The crystallization slurry was aged for 24 h, and the resulting slurry was filtered to isolate the solid. The cake was washed twice with water (2× 3.8 mL) before being dried under reduced pressure at <50 °C to provide **18** (1.82 g) as a tan powder in 69.9% yield. ^{1}H NMR (400 MHz, DMSO-d_6) δ 15.00−14.88 (m, 1H), 11.94 (br s, 1H), 11.78 (s, 1H), 10.89 (br s, 1H), 8.54 (d, J = 2.4 Hz, 1H), 7.92−7.85 (m, 1H), 7.45 (d, J = 8.4 Hz, 1H), 7.35 (t, J = 8.4 Hz, 1H), 6.71 (d, J = 8.4 Hz, 2H), 3.97 (s, 2H), 3.79 (s, 2H), 3.68 (s, 6H), 3.26 (q, J = 7.0 Hz, 2H), 0.98 (t, J = 7.0 Hz, 3H). ^{13}C NMR (101 MHz,

https://doi.org/10.1021/acs.oprd.1c00088
Org. Process Res. Dev. XXXX, XXX, XXX−XXX

DMSO-d_6) δ 171.7, 166.4, 164.9, 160.7, 156.5, 152.5, 145.8, 145.8, 134.7, 128.6, 127.8, 123.7, 106.4, 104.2, 102.4, 94.5, 64.0, 63.8, 54.0, 40.1, 13.1. HRMS $[M + H]^+$ calcd for $C_{24}H_{25}ClN_4O_7$ 517.1485, found 517.1494.

■ ASSOCIATED CONTENT

Supporting Information

The Supporting Information is available free of charge at https://pubs.acs.org/doi/10.1021/acs.oprd.1c00088.

Experimental details, characterization data, NMR spectra, and HRMS spectra (PDF)

■ AUTHOR INFORMATION

Corresponding Author

Matthew J. Goldfogel − *Chemical Process Development, Bristol Myers Squibb, New Brunswick, New Jersey 08903, United States;* orcid.org/0000-0002-6911-3068; Email: matthew.goldfogel@bms.com

Authors

Christopher R. Jamison − *Chemical Process Development, Bristol Myers Squibb, New Brunswick, New Jersey 08903, United States*

Scott A. Savage − *Chemical Process Development, Bristol Myers Squibb, New Brunswick, New Jersey 08903, United States;* orcid.org/0000-0002-7823-0696

Matthew W. Haley − *Chemical Process Development, Bristol Myers Squibb, New Brunswick, New Jersey 08903, United States*

Subha Mukherjee − *Chemical Process Development, Bristol Myers Squibb, New Brunswick, New Jersey 08903, United States*

Chris Sfouggatakis − *Chemical Process Development, Bristol Myers Squibb, New Brunswick, New Jersey 08903, United States*

Manjunath Gujjar − *Chemical Development and API Supply, Biocon Bristol Myers Squibb Research and Development Center, Bangalore 560 099, India*

Jayaraj Mohan − *Chemical Development and API Supply, Biocon Bristol Myers Squibb Research and Development Center, Bangalore 560 099, India*

Souvik Rakshit − *Chemical Development and API Supply, Biocon Bristol Myers Squibb Research and Development Center, Bangalore 560 099, India*

Rajappa Vaidyanathan − *Chemical Development and API Supply, Biocon Bristol Myers Squibb Research and Development Center, Bangalore 560 099, India;* orcid.org/0000-0002-2236-5719

Complete contact information is available at: https://pubs.acs.org/10.1021/acs.oprd.1c00088

Notes

The authors declare no competing financial interest.

■ ACKNOWLEDGMENTS

The authors are thankful for the insight and assistance of Dr. Heather Finlay in understanding the biochemistry of the APJ receptor. The authors would like to thank the Isolation and Structural Elucidation group at Bristol Myers Squibb (New Brunswick, NJ) for their analytical support.

■ REFERENCES

(1) Benjamin, E. J.; Muntner, P.; Alonso, A.; Bittencourt, M. S.; Callaway, C. W.; Carson, A. P.; Chamberlain, A. M.; Chang, A. R.; Cheng, S.; Das, S. R.; Delling, F. N.; Djousse, L.; Elkind, M. S. V.; Ferguson, J. F.; Fornage, M.; Jordan, L. C.; Khan, S. S.; Kissela, B. M.; Knutson, K. L.; Kwan, T. W.; Lackland, D. T.; Lewis, T. T.; Lichtman, J. H.; Longenecker, C. T.; Loop, M. S.; Lutsey, P. L.; Martin, S. S.; Matsushita, K.; Moran, A. E.; Mussolino, M. E.; O'Flaherty, M.; Pandey, A.; Perak, A. M.; Rosamond, W. D.; Roth, G. A.; Sampson, U. K. A.; Satou, G. M.; Schroeder, E. B.; Shah, S. H.; Spartano, N. L.; Stokes, A.; Tirschwell, D. L.; Tsao, C. W.; Turakhia, M. P.; VanWagner, L. B.; Wilkins, J. T.; Wong, S. S.; Virani, S. S. Heart Disease and Stroke Statistics—2019 Update: A Report From the American Heart Association. *Circulation* **2019**, *139* (10), 56−528.

(2) Ponikowski, P.; Anker, S. D.; AlHabib, K. F.; Cowie, M. R.; Force, T. L.; Hu, S.; Jaarsma, T.; Krum, H.; Rastogi, V.; Rohde, L. E.; Samal, U. C.; Shimokawa, H.; Budi Siswanto, B.; Sliwa, K.; Filippatos, G. Heart Failure: Preventing Disease and Death Worldwide. *ESC Heart Fail.* **2014**, *1* (1), 4−25.

(3) Roger, V. L.; Weston, S. A.; Redfield, M. M.; Hellermann-Homan, J. P.; Killian, J.; Yawn, B. P.; Jacobsen, S. J. Trends in Heart Failure Incidence and Survival in a Community-Based Population. *JAMA* **2004**, *292* (3), 344−350.

(4) Roger, V. L. Epidemiology of Heart Failure. *Circ. Res.* **2013**, *113* (6), 646−659.

(5) O'Dowd, B. F.; Heiber, M.; Chan, A.; Heng, H. H.; Tsui, L. C.; Kennedy, J. L.; Shi, X.; Petronis, A.; George, S. R.; Nguyen, T. A Human Gene That Shows Identity with the Gene Encoding the Angiotensin Receptor Is Located on Chromosome 11. *Gene* **1993**, *136* (1−2), 355−360.

(6) Kuba, K.; Sato, T.; Imai, Y.; Yamaguchi, T. Apelin and Elabela/Toddler; Double Ligands for APJ/Apelin Receptor in Heart Development, Physiology, and Pathology. *Peptides* **2019**, *111*, 62−70.

(7) Folino, A.; Montarolo, P. G.; Samaja, M.; Rastaldo, R. Effects of Apelin on the Cardiovascular System. *Heart Failure Rev.* **2015**, *20* (4), 505−518.

(8) Tatemoto, K.; Hosoya, M.; Habata, Y.; Fujii, R.; Kakegawa, T.; Zou, M. X.; Kawamata, Y.; Fukusumi, S.; Hinuma, S.; Kitada, C.; Kurokawa, T.; Onda, H.; Fujino, M. Isolation and Characterization of a Novel Endogenous Peptide Ligand for the Human APJ Receptor. *Biochem. Biophys. Res. Commun.* **1998**, *251* (2), 471−476.

(9) Ma, Y.; Yue, Y.; Ma, Y.; Zhang, Q.; Zhou, Q.; Song, Y.; Shen, Y.; Li, X.; Ma, X.; Li, C.; Hanson, M. A.; Han, G. W.; Sickmier, E. A.; Swaminath, G.; Zhao, S.; Stevens, R. C.; Hu, L. A.; Zhong, W.; Zhang, M.; Xu, F. Structural Basis for Apelin Control of the Human Apelin Receptor. *Structure* **2017**, *25* (6), 858−866.

(10) Maguire, J. J.; Kleinz, M. J.; Pitkin, S. L.; Davenport, A. P. [Pyr1]Apelin-13 Identified as the Predominant Apelin Isoform in the Human Heart: Vasoactive Mechanisms and Inotropic Action in Disease. *Hypertension* **2009**, *54* (3), 598−604.

(11) Zhen, E. Y.; Higgs, R. E.; Gutierrez, J. A. Pyroglutamyl Apelin-13 Identified as the Major Apelin Isoform in Human Plasma. *Anal. Biochem.* **2013**, *442* (1), 1−9.

(12) Japp, A. G.; Cruden, N. L.; Barnes, G.; van Gemeren, N.; Mathews, J.; Adamson, J.; Johnston, N. R.; Denvir, M. A.; Megson, I. L.; Flapan, A. D.; Newby, D. E. Acute Cardiovascular Effects of Apelin in Humans. *Circulation* **2010**, *121* (16), 1818−1827.

(13) Boal, F.; Timotin, A.; Roumegoux, J.; Alfarano, C.; Calise, D.; Anesia, R.; Parini, A.; Valet, P.; Tronchere, H.; Kunduzova, O. Apelin-13 Administration Protects against Ischaemia/Reperfusion-Mediated Apoptosis through the FoxO1 Pathway in High-Fat Diet-Induced Obesity. *Br. J. Pharmacol.* **2016**, *173* (11), 1850−1863.

(14) Pang, H.; Han, B.; Yu, T.; Zong, Z. Effect of Apelin on the Cardiac Hemodynamics in Hypertensive Rats with Heart Failure. *Int. J. Mol. Med.* **2014**, *34* (3), 756−764.

(15) Barnes, G. D.; Alam, S.; Carter, G.; Pedersen, C. M.; Lee, K. M.; Hubbard, T. J.; Veitch, S.; Jeong, H.; White, A.; Cruden, N. L.; Huson, L.; Japp, A. G.; Newby, D. E. Sustained Cardiovascular Actions of APJ Agonism during Renin-Angiotensin System Activation

and in Patients with Heart Failure. *Circ.: Heart Failure* **2013**, *6* (3), 482−491.
(16) Japp, A. G.; Cruden, N. L.; Amer, D. A. B.; Li, V. K. Y.; Goudie, E. B.; Johnston, N. R.; Sharma, S.; Neilson, I.; Webb, D. J.; Megson, I. L.; Flapan, A. D.; Newby, D. E. Vascular Effects of Apelin In Vivo in Man. *J. Am. Coll. Cardiol.* **2008**, *52* (11), 908−913.
(17) Su, S.; Clarke, A.; Han, Y.; Chao, H. J.; Bostwick, J.; Schumacher, W.; Wang, T.; Yan, M.; Hsu, M.-Y.; Simmons, E.; Luk, C.; Xu, C.; Dabros, M.; Galella, M.; Onorato, J.; Gordon, D.; Wexler, R.; Gargalovic, P. S.; Lawrence, R. M. Biphenyl Acid Derivatives as APJ Receptor Agonists. *J. Med. Chem.* **2019**, *62* (22), 10456−10465.
(18) Jia, Z. Q.; Hou, L.; Leger, A.; Wu, I.; Kudej, A. B.; Stefano, J.; Jiang, C.; Pan, C. Q.; Akita, G. Y. Cardiovascular Effects of a PEGylated Apelin. *Peptides* **2012**, *38* (1), 181−188.
(19) Brame, A. L.; Maguire, J. J.; Yang, P.; Dyson, A.; Torella, R.; Cheriyan, J.; Singer, M.; Glen, R. C.; Wilkinson, I. B.; Davenport, A. P. Design, Characterization, and First-in-Human Study of the Vascular Actions of a Novel Biased Apelin Receptor Agonist. *Hypertension* **2015**, *65* (4), 834−840.
(20) Narayanan, S.; Maitra, R.; Deschamps, J. R.; Bortoff, K.; Thomas, J. B.; Zhang, Y.; Warner, K.; Vasukuttan, V.; Decker, A.; Runyon, S. P. Discovery of a Novel Small Molecule Agonist Scaffold for the APJ Receptor. *Bioorg. Med. Chem.* **2016**, *24* (16), 3758−3770.
(21) Narayanan, S.; Harris, D. L.; Maitra, R.; Runyon, S. P. Regulation of the Apelinergic System and Its Potential in Cardiovascular Disease: Peptides and Small Molecules as Tools for Discovery. *J. Med. Chem.* **2015**, *58* (20), 7913−7927.
(22) McKinnie, S. M. K.; Wang, W.; Fischer, C.; McDonald, T.; Kalin, K. R.; Iturrioz, X.; Llorens-Cortes, C.; Oudit, G. Y.; Vederas, J. C. Synthetic Modification within the "RPRL" Region of Apelin Peptides: Impact on Cardiovascular Activity and Stability to Neprilysin and Plasma Degradation. *J. Med. Chem.* **2017**, *60* (14), 6408−6427.
(23) McKeown, S. C.; Zecri, F. J.; Fortier, E.; Taggart, A.; Sviridenko, L.; Adams, C. M.; McAllister, K. H.; Pin, S. S. The Design and Implementation of a Generic Lipopeptide Scanning Platform to Enable the Identification of "locally Acting" Agonists for the Apelin Receptor. *Bioorg. Med. Chem. Lett.* **2014**, *24* (20), 4871−4875.
(24) Myers, M. C.; Bilder, D. M.; Cavallaro, C. L.; Chao, H. J.; Su, S.; Burford, N. T.; Nayeem, A.; Wang, T.; Yan, M.; Langish, R. A.; Dabros, M.; Li, Y.-X.; Rose, A. V.; Behnia, K.; Onorato, J. M.; Gargalovic, P. S.; Wexler, R. R.; Lawrence, R. M. Discovery and SAR of Aryl Hydroxy Pyrimidinones as Potent Small Molecule Agonists of the GPCR APJ. *Bioorg. Med. Chem. Lett.* **2020**, *30* (7), 126955.
(25) Gargalovic, P.; Wong, P.; Onorato, J.; Finlay, H.; Wang, T.; Yan, M.; Crain, E.; St-Onge, S.; Héroux, M.; Bouvier, M. In Vitro and in Vivo Evaluation of a Small-Molecule APJ (Apelin Receptor) Agonist, BMS-986224, as a Potential Treatment for Heart Failure. *Circ.: Heart Failure* **2021**, *14*, No. e007351.
(26) Bristol-Myers Squibb. *A Randomized, Double-Blinded, Placebo-Controlled, Single and Multiple Ascending Dose Study to Evaluate the Safety, Tolerability, Pharmacokinetics and Pharmacodynamics of BMS-986224 in Healthy Subjects and Chronic Heart Failure Patients With Reduced Ejection Fraction; Clinical trial registration NCT03281122*; clinicaltrials.gov, 2020.
(27) Collins, D. J.; James, A. M. 4-(6'-Methoxy-3′,4'-Dihydronaphthalen-1'-Yl)Butan-2-One and the Derived Guareschi Imide. *Aust. J. Chem.* **1989**, *42* (1), 215−221.
(28) Baron, H.; Remfry, F. G. P.; Thorpe, J. F. The Formation and Reactions of Imino-Compounds. Part I. Condensation of Ethyl Cyanoacetate with Its Sodium Derivative. *J. Chem. Soc., Trans.* **1904**, *85* (0), 1726−1761.
(29) Jaiswal, P. K.; Sharma, V.; Mathur, M.; Chaudhary, S. Organocatalytic Modified Guareschi-Thorpe Type Regioselective Synthesis: A Unified Direct Access to 5,6,7,8-Tetrahydroquinolines and Other Alicyclic[b]-Fused Pyridines. *Org. Lett.* **2018**, *20* (19), 6059−6063.
(30) McDaniel, K. F.; Wang, L.; Soltwedel, T.; Fidanze, S. D.; Hasvold, L. A.; Liu, D.; Mantei, R. A.; Pratt, J. K.; Sheppard, G. S.; Bui, M. H.; Faivre, E. J.; Huang, X.; Li, L.; Lin, X.; Wang, R.; Warder, S. E.; Wilcox, D.; Albert, D. H.; Magoc, T. J.; Rajaraman, G.; Park, C. H.; Hutchins, C. W.; Shen, J. J.; Edalji, R. P.; Sun, C. C.; Martin, R.; Gao, W.; Wong, S.; Fang, G.; Elmore, S. W.; Shen, Y.; Kati, W. M. Discovery of N-(4-(2,4-Difluorophenoxy)-3-(6-Methyl-7-Oxo-6,7-Dihydro-1H-Pyrrolo[2,3-c]Pyridin-4-Yl)Phenyl)Ethanesulfonamide (ABBV-075/Mivebresib), a Potent and Orally Available Bromodomain and Extraterminal Domain (BET) Family Bromodomain Inhibitor. *J. Med. Chem.* **2017**, *60* (20), 8369−8384.
(31) Zhang, Z.; Liu, C.; Li, X.; Song, T.; Wu, Z.; Liang, X.; Zhao, Y.; Shen, X.; Chen, H. Fragment-Based Design, Synthesis, and Biological Evaluation of N-Substituted-5-(4-Isopropylthiophenol)-2-Hydroxynicotinamide Derivatives as Novel Mcl-1 Inhibitors. *Eur. J. Med. Chem.* **2013**, *60*, 410−420.
(32) Awuah, E.; Capretta, A. Strategies and Synthetic Methods Directed Toward the Preparation of Libraries of Substituted Isoquinolines. *J. Org. Chem.* **2010**, *75* (16), 5627−5634.
(33) Jessen, H. J.; Schumacher, A.; Shaw, T.; Pfaltz, A.; Gademann, K. A Unified Approach for the Stereoselective Total Synthesis of Pyridone Alkaloids and Their Neuritogenic Activity. *Angew. Chem., Int. Ed.* **2011**, *50* (18), 4222−4226.
(34) Zhang, A.; Ding, C.; Cheng, C.; Yao, Q. Convenient Synthesis of 2,7-Naphthyridine Lophocladines A and B and Their Analogues. *J. Comb. Chem.* **2007**, *9* (6), 916−919.
(35) Khadka, D. B.; Woo, H.; Yang, S. H.; Zhao, C.; Jin, Y.; Le, T. N.; Kwon, Y.; Cho, W.-J. Modification of 3-Arylisoquinolines into 3,4-Diarylisoquinolines and Assessment of Their Cytotoxicity and Topoisomerase Inhibition. *Eur. J. Med. Chem.* **2015**, *92*, 583−607.
(36) Ali, N. M.; McKillop, A.; Mitchell, M. B.; Rebelo, R. A.; Wallbank, P. J. Palladium-Catalysed Cross-Coupling Reactions of Arylboronic Acids with π-Deficient Heteroaryl Chlorides. *Tetrahedron* **1992**, *48* (37), 8117−8126.
(37) Hasvold, L. A.; Wang, W.; Gwaltney, S. L.; Rockway, T. W.; Nelson, L. T. J.; Mantei, R. A.; Fakhoury, S. A.; Sullivan, G. M.; Li, Q.; Lin, N.-H.; Wang, L.; Zhang, H.; Cohen, J.; Gu, W.-Z.; Marsh, K.; Bauch, J.; Rosenberg, S.; Sham, H. L. Pyridone-Containing Farnesyltransferase Inhibitors: Synthesis and Biological Evaluation. *Bioorg. Med. Chem. Lett.* **2003**, *13* (22), 4001−4005.
(38) Smyth, L. A.; Matthews, T. P.; Horton, P. N.; Hursthouse, M. B.; Collins, I. Synthesis and Reactivity of 3-Amino-1H-Pyrazolo[4,3-c]Pyridin-4(5H)-Ones: Development of a Novel Kinase-Focussed Library. *Tetrahedron* **2010**, *66* (15), 2843−2854.
(39) Fu, W. C.; Zhou, Z.; Kwong, F. Y. A Benzo[c]Carbazolyl-Based Phosphine Ligand for Pd-Catalyzed Tetra-Ortho-Substituted Biaryl Syntheses. *Org. Chem. Front.* **2016**, *3* (2), 273−276.
(40) Zhao, Q.; Li, C.; Senanayake, C. H.; Tang, W. An Efficient Method for Sterically Demanding Suzuki-Miyaura Coupling Reactions. *Chem. - Eur. J.* **2013**, *19* (7), 2261−2265.
(41) Hoshi, T.; Nakazawa, T.; Saitoh, I.; Mori, A.; Suzuki, T.; Sakai, J.; Hagiwara, H. Biphenylene-Substituted Ruthenocenylphosphine for Suzuki-Miyaura Coupling of Aryl Chlorides. *Org. Lett.* **2008**, *10* (10), 2063−2066.
(42) Barder, T. E.; Walker, S. D.; Martinelli, J. R.; Buchwald, S. L. Catalysts for Suzuki-Miyaura Coupling Processes: Scope and Studies of the Effect of Ligand Structure. *J. Am. Chem. Soc.* **2005**, *127* (13), 4685−4696.
(43) Patel, N. D.; Sieber, J. D.; Tcyrulnikov, S.; Simmons, B. J.; Rivalti, D.; Duvvuri, K.; Zhang, Y.; Gao, D. A.; Fandrick, K. R.; Haddad, N.; Lao, K. S.; Mangunuru, H. P. R.; Biswas, S.; Qu, B.; Grinberg, N.; Pennino, S.; Lee, H.; Song, J. J.; Gupton, B. F.; Garg, N. K.; Kozlowski, M. C.; Senanayake, C. H. Computationally Assisted Mechanistic Investigation and Development of Pd-Catalyzed Asymmetric Suzuki-Miyaura and Negishi Cross-Coupling Reactions for Tetra-Ortho-Substituted Biaryl Synthesis. *ACS Catal.* **2018**, *8* (11), 10190−10209.
(44) Yang, H.; Sun, J.; Gu, W.; Tang, W. Enantioselective Cross-Coupling for Axially Chiral Tetra-Ortho-Substituted Biaryls and Asymmetric Synthesis of Gossypol. *J. Am. Chem. Soc.* **2020**, *142* (17), 8036−8043.

https://doi.org/10.1021/acs.oprd.1c00088
Org. Process Res. Dev. XXXX, XXX, XXX−XXX

(45) Giannerini, M.; Hornillos, V.; Vila, C.; Fañanás-Mastral, M.; Feringa, B. L. Hindered Aryllithium Reagents as Partners in Palladium-Catalyzed Cross-Coupling: Synthesis of Tri- and Tetra-Ortho-Substituted Biaryls under Ambient Conditions. *Angew. Chem., Int. Ed.* **2013**, *52* (50), 13329−13333.
(46) Yuen, O. Y.; Leung, M. P.; So, C. M.; Sun, R. W.-Y.; Kwong, F. Y. Palladium-Catalyzed Direct Arylation of Polyfluoroarenes for Accessing Tetra-Ortho-Substituted Biaryls: Buchwald-Type Ligand Having Complementary -PPh2Moiety Exhibits Better Efficiency. *J. Org. Chem.* **2018**, *83* (16), 9008−9017.
(47) Chartoire, A.; Lesieur, M.; Falivene, L.; Slawin, A. M. Z.; Cavallo, L.; Cazin, C. S. J.; Nolan, S. P. [Pd(IPr*)(Cinnamyl)Cl]: An Efficient Pre-Catalyst for the Preparation of Tetra-Ortho-Substituted Biaryls by Suzuki-Miyaura Cross-Coupling. *Chem. - Eur. J.* **2012**, *18* (15), 4517−4521.
(48) So, C. M.; Chow, W. K.; Choy, P. Y.; Lau, C. P.; Kwong, F. Y. Remarkably Effective Phosphanes Simply with a PPh2Moiety: Application to Pd-Catalysed Cross-Coupling Reactions for Tetra-Ortho-Substituted Biaryl Syntheses. *Chem. - Eur. J.* **2010**, *16* (27), 7996−8001.
(49) Wu, L.; Drinkel, E.; Gaggia, F.; Capolicchio, S.; Linden, A.; Falivene, L.; Cavallo, L.; Dorta, R. Room-Temperature Synthesis of Tetra-Ortho-Substituted Biaryls by NHC-Catalyzed Suzuki-Miyaura Couplings. *Chem. - Eur. J.* **2011**, *17* (46), 12886−12890.
(50) Li, G.-Q.; Yamamoto, Y.; Miyaura, N. Synthesis of Tetra-Ortho-Substituted Biaryls Using Aryltriolborates. *Synlett* **2011**, *2011* (12), 1769−1773.
(51) Ackermann, L.; Potukuchi, H. K.; Althammer, A.; Born, R.; Mayer, P. Tetra-Ortho-Substituted Biaryls through Palladium-Catalyzed Suzuki-Miyaura Couplings with a Diaminochlorophosphine Ligand. *Org. Lett.* **2010**, *12* (5), 1004−1007.
(52) McKnelly, K. J.; Sokol, W.; Nowick, J. S. Anaphylaxis Induced by Peptide Coupling Agents: Lessons Learned from Repeated Exposure to HATU, HBTU, and HCTU. *J. Org. Chem.* **2020**, *85* (3), 1764−1768.
(53) Beutner, G. L.; Young, I. S.; Davies, M. L.; Hickey, M. R.; Park, H.; Stevens, J. M.; Ye, Q. TCFH-NMI: Direct Access to N-Acyl Imidazoliums for Challenging Amide Bond Formations. *Org. Lett.* **2018**, *20* (14), 4218−4222.
(54) Andraos, J. Aiming for a Standardized Protocol for Preparing a Process Green Synthesis Report and for Ranking Multiple Synthesis Plans to a Common Target Product. *Green Process. Synth.* **2019**, *8* (1), 787−801.
(55) Li, J.; Eastgate, M. D. Making Better Decisions during Synthetic Route Design: Leveraging Prediction to Achieve Greenness-by-Design. *React. Chem. Eng.* **2019**, *4* (9), 1595−1607.
(56) Monteith, E. R.; Mampuys, P.; Summerton, L.; Clark, J. H.; Maes, B. U. W.; McElroy, C. R. Why We Might Be Misusing Process Mass Intensity (PMI) and a Methodology to Apply It Effectively as a Discovery Level Metric. *Green Chem.* **2020**, *22* (1), 123−135.
(57) Ohashi, T.; Oguro, Y.; Tanaka, T.; Shiokawa, Z.; Tanaka, Y.; Shibata, S.; Sato, Y.; Yamakawa, H.; Hattori, H.; Yamamoto, Y.; Kondo, S.; Miyamoto, M.; Nishihara, M.; Ishimura, Y.; Tojo, H.; Baba, A.; Sasaki, S. Discovery of the Investigational Drug TAK-441, a Pyrrolo[3,2-c]Pyridine Derivative, as a Highly Potent and Orally Active Hedgehog Signaling Inhibitor: Modification of the Core Skeleton for Improved Solubility. *Bioorg. Med. Chem.* **2012**, *20* (18), 5507−5517.
(58) Cao, Y.; Zhang, Y.; Wu, S.; Yang, Q.; Sun, X.; Zhao, J.; Pei, F.; Guo, Y.; Tian, C.; Zhang, Z.; Wang, H.; Ma, L.; Liu, J.; Wang, X. Synthesis and Biological Evaluation of Pyridinone Analogues as Novel Potent HIV-1 NNRTIs. *Bioorg. Med. Chem.* **2015**, *23* (1), 149−159.
(59) Mittelbach, M.; Schmidt, H.-W.; Uray, G.; Junek, H.; Lamm, B.; Ankner, K.; Brändström, A.; Simonsson, R. Synthesis of 4-Methoxy-2,3,5-Trimethylpyridine: A Specific Building Block for Compounds with Gastric-Acid Inhibiting Activity. *Acta Chem. Scand.* **1988**, *42b*, 524−529.
(60) Striela, R.; Urbelis, G.; Sūdžius, J.; Stončius, S.; Mažeikaitė, R.; Labanauskas, L. Total Synthesis of S-Hydroxyomeprazole. *ARKIVOC* **2016**, *2016* (3), 339.
(61) Mukhopadhyay, S.; Batra, S. Applications of Sodium Nitrite in Organic Synthesis. *Eur. J. Org. Chem.* **2019**, *2019* (38), 6424−6451.
(62) Selekman, J. A.; Qiu, J.; Tran, K.; Stevens, J.; Rosso, V.; Simmons, E.; Xiao, Y.; Janey, J. High-Throughput Automation in Chemical Process Development. *Annu. Rev. Chem. Biomol. Eng.* **2017**, *8* (1), 525−547.
(63) Schmink, J.; Bellomo, A.; Berritt, S. Scientist-Led High-Throughput Experimentation (HTE) and Its Utility in Academia and Industry. *Aldrichimica Acta* **2013**, *46*, 71−80.
(64) Orr, S. T. M.; Beveridge, R.; Bhattacharya, S. K.; Cameron, K. O.; Coffey, S.; Fernando, D.; Hepworth, D.; Jackson, M. V.; Khot, V.; Kosa, R.; Lapham, K.; Loria, P. M.; McClure, K. F.; Patel, J.; Rose, C.; Saenz, J.; Stock, I. A.; Storer, G.; von Volkenburg, M.; Vrieze, D.; Wang, G.; Xiao, J.; Zhang, Y. Evaluation and Synthesis of Polar Aryl- and Heteroaryl Spiroazetidine-Piperidine Acetamides as Ghrelin Inverse Agonists. *ACS Med. Chem. Lett.* **2015**, *6* (2), 156−161.

https://doi.org/10.1021/acs.oprd.1c00088
Org. Process Res. Dev. XXXX, XXX, XXX−XXX